Maximum-performance fiber-optic irradiation with nonimaging designs

Yueping Fang, Daniel Feuermann, and J. M. Gordon

A range of practical nonimaging designs for optical fiber applications is presented. Rays emerging from a fiber over a restricted angular range (small numerical aperture) are needed to illuminate a small near-field detector at maximum radiative efficiency. These designs range from pure reflector (all-mirror), to pure dielectric (refractive and based on total internal reflection) to lens–mirror combinations. Sample designs are shown for a specific infrared fiber-optic irradiation problem of practical interest. Optical performance is checked with computer three-dimensional ray tracing. Compared with conventional imaging solutions, nonimaging units offer considerable practical advantages in compactness and ease of alignment as well as noticeably superior radiative efficiency. © 1997 Optical Society of America

1. Introduction

Nonimaging optics offer optical designs that are uniquely well suited to fiber-optic applications.[1] Consider delivering light emitted from an optical fiber onto a near-field target, such that close to 100% of the emitted light strikes the detector. Our specific practical uses are for (a) infrared optical fibers of small numerical aperture (limited field of view for the bundle of rays emitted); (b) a detector area that is not much larger than the fiber's cross-sectional area and not necessarily of the same shape; and (c) a finite fiber-to-detector distance, as drawn schematically in Fig. 1. Applications include radiometry, infrared spectroscopy, evanescent wave spectroscopy (also commonly referred to as attenuated total reflection spectroscopy), and material characterization.[2–4] In fact, the devices developed in this paper are currently being prepared for new laser fiber-optic ear surgical procedures.[5]

What makes the development of practical nonimaging devices particularly challenging is the severely restricted exit angle from the fiber, the small size of the target (and the requirement that close to 0% of the emitted power falls outside the detector), and the small angle subtended from the fiber to the target. Such constraints usually dictate nonimaging devices that are inordinately long (deep) compared with the fiber diameter. Nonetheless we will demonstrate that several different classes of nonimaging designs provide feasible solutions.

Equally important, these nonimaging systems are superior in radiative efficiency to conventional imaging units, such as spherical lenses or ellipsoidal mirrors. The key reason is that imaging systems inherently place a substantial fraction of the emitted rays outside the target area to accommodate the angular and the dimensional constraints. Nonimaging devices, designed according to the edge-ray principle,[1,6] ensure that extreme rays strike the target, so that all intermediate rays are accommodated, albeit at considerable loss in image quality. In our applications, sharp image formation is irrelevant; only maximum-efficiency radiation transmission matters. Also note that our analyses fall within the realm of geometric optics, an excellent approximation since the wavelength of the radiation is of the order of 10^{-3}–10^{-2} mm, whereas fiber diameters are near 1 mm.

Furthermore imaging systems of acceptably high radiative efficiency are physically large, e.g., in the distances between fiber, optical element (e.g., ellipsoidal mirror or spherical lens), and detector, and in the size of the imaging optical element. The nonimaging devices developed here are typically much smaller than the corresponding imaging solutions and attach directly onto the tip of the optical fiber. System dimensions can be reduced by more than an

The authors are with the Center for Energy and Environmental Physics, Jacob Blaustein Institute for Desert Research, Ben-Gurion University of the Negev, Sede Boqer Campus 84990, Israel. J. M. Gordon is also with the Department of Mechanical Engineering, Pearlstone Center for Aeronautical Engineering Studies, Ben-Gurion University of the Negev, Beersheva 84105, Israel.

Received 4 February 1997; revised manuscript received 1 May 1997.

0003-6935/97/07107-07$10.00/0

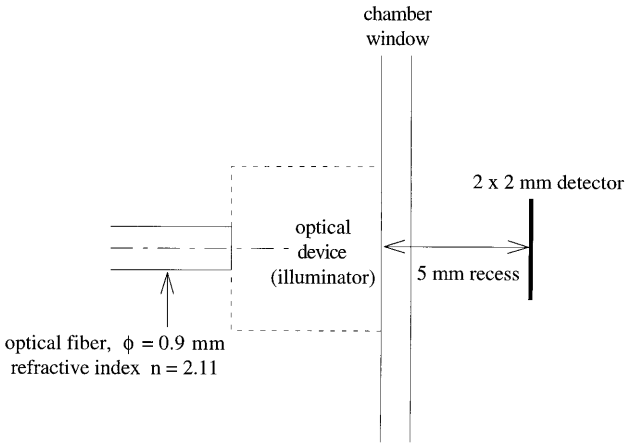

Fig. 1. Cross section of the system configuration for our design exercises. The optical fiber has an active core diameter of 0.9 mm, a refractive index of 2.11, and an angular extent within the fiber of ±11.55°. A standard square 2 mm × 2 mm detector sits within a chamber and must be recessed 5 mm from the chamber window. Some optical device is to be placed on the fiber tip, exterior to the chamber, so as to project radiation onto the target.

order of magnitude. In addition, the imaging assembly requires two precision alignments (fiber to optical element and optical element to target), whereas our nonimaging elements require only one alignment because the fiber and the optical element form a single unit.

Our nonimaging solutions include (1) all-mirror (pure specular reflective) designs; (2) all-dielectric (pure refractive, total-internal-reflection) designs; and (3) lens–mirror combinations. Each class offers its own set of practical virtues. Toward illustrating our solutions in concrete terms, we focus on a particular set of practical material properties and a specific system configuration.[3–5] Scale drawings of promising designs are presented along with performance estimates based on computer three-dimensional (3D) ray-trace simulation results.

Our designs are variations on a theme of classical nonimaging solutions that were originally developed to concentrate radiation to the thermodynamic limit.[1,7] In our illumination problem, the roles of source and target are interchanged relative to the concentration problem. The variations refer to our designing for (i) highly restricted angular ranges of both incident and emitted rays and (ii) a small, near-field target.

2. System Parameters

The infrared optical fibers are made from crystalline silver halide alloys ($AgCl_xBr_{1-x}$), are unclad, have a diameter of 0.9 mm, and have a refractive index n = 2.11 with excellent transmissivity for the middle infrared (wavelength range of 2–25 μm).[3–5] The fiber ends are flat disks and can include an antireflective coating to reduce Fresnel reflection losses. The optical designs delineated here are equally applicable to clad fibers, provided the entrance aperture of our irradiators is placed flush against the fiber core and has the same area and shape as that core.

The particular set of applications considered here has radiation propagating within the fiber over an angular extent of ±11.55°, such that if the rays are emitted into air (n = 1.0) from a flat fiber end, the angular extent increases to ±25.0°. The 11.55° and 25.0° values must serve as the restricted entrance angle for our nonimaging designs, depending on whether a dielectric or a mirror element is attached to the fiber tip.

Placed in a cooled low-pressure chamber, a standard square 2 mm × 2 mm infrared detector is recessed from the chamber window. The requirements of the plane of the exit aperture of any device we design must be no closer than 5 mm to the plane of the detector (Fig. 1).

What creates a challenging practical nonimaging design problem is that the angle subtended by the detector from the exit aperture of our irradiation device (whatever it turns out to be) is not much smaller than the restricted entrance angle to the device. Furthermore, the exit aperture diameter is limited by the detector area. Nonimaging irradiators are phase-space transformers,[1] namely, they convert an incident bundle of rays that covers a given area and a projected solid angle into an outgoing bundle of larger area but of smaller projected solid angle. The key constraint we impose is that this transformation be effected such that almost no rays miss the target. To accommodate such a transformation for the system parameters imposed here, nonimaging devices turn out to be deep (relative to the source diameter). Besides pointing out why this disadvantage might not be excessively deleterious for fiber-optic uses, we also develop reasonably compact solutions.

3. Pure Reflective, All-Mirror Devices

As in all the designs offered here, we exploit the edge-ray principle[1,6] to motivate the solution. Since solutions are developed for the corresponding two-dimensional (2D) (linear) systems, we proceed by solving the 2D problem exactly and then rotating these cross sections to produce axially symmetric 3D devices. Since there is no guarantee that skew rays will be accommodated too, and since there are no known analytic procedures for checking the rejection of skew rays, we verify the system performance with a computer 3D ray-trace simulation. Since the designs are axially symmetric, we will describe the construction for the right-hand-side profile only (FDB in Figs. 2–4). The left-hand-side profile is simply its mirror image.

Our light source is approximated as quasi-Lambertian, emitting uniformly in position over its surface and uniformly in angle, but only within the angular cutoff noted above. The manner in which optical performance changes when this approximation is relaxed, that is, system behavior for an inhomogeneous light source, is addressed in Section 7.

Consider the extreme rays emitted from point A (Fig. 2). The restricted numerical aperture of the problem dictates that these rays emerge into air at angles not exceeding 25.0°. We start the design

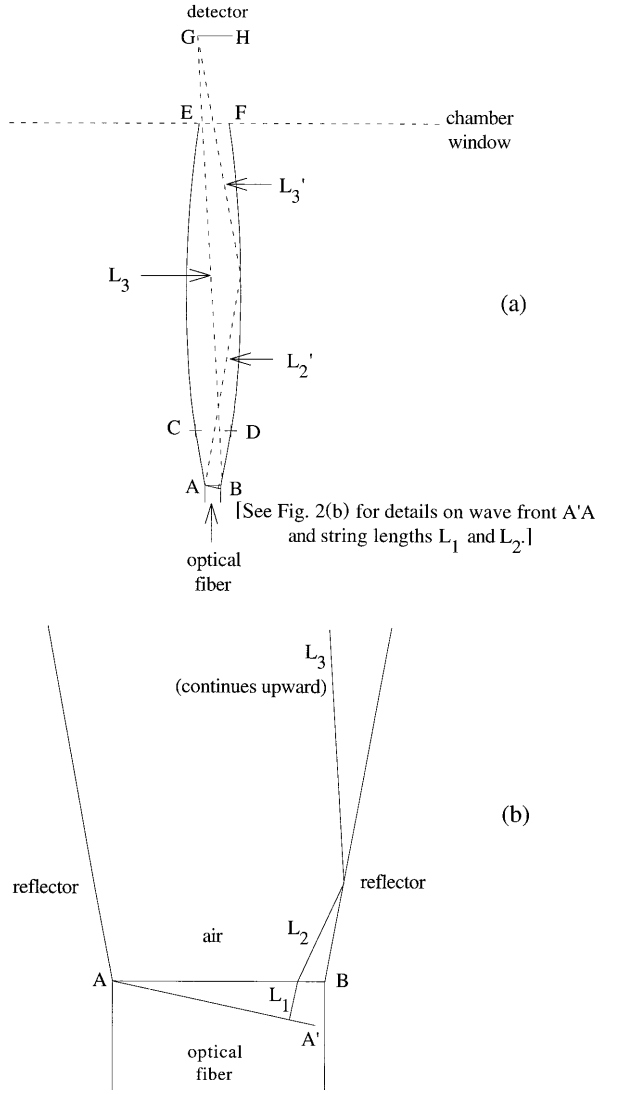

Fig. 2. Design of the all-mirror (pure-reflective) nonimaging unit, in 2D cross section. Rays emerge from fiber tip AB into air over an angular range of $\pm 25.0°$. Reflector design is described in the text, such that section FD is a rotated elliptical arc with ellipse foci at A and G. Section DB is a rotated parabolic arc with parabola focus at G and parabola axis parallel to rays from the extreme wave front $A'A$. String lengths are denoted by L: (a) full view; (b) zoom on entrance aperture to show details of string lengths in that region.

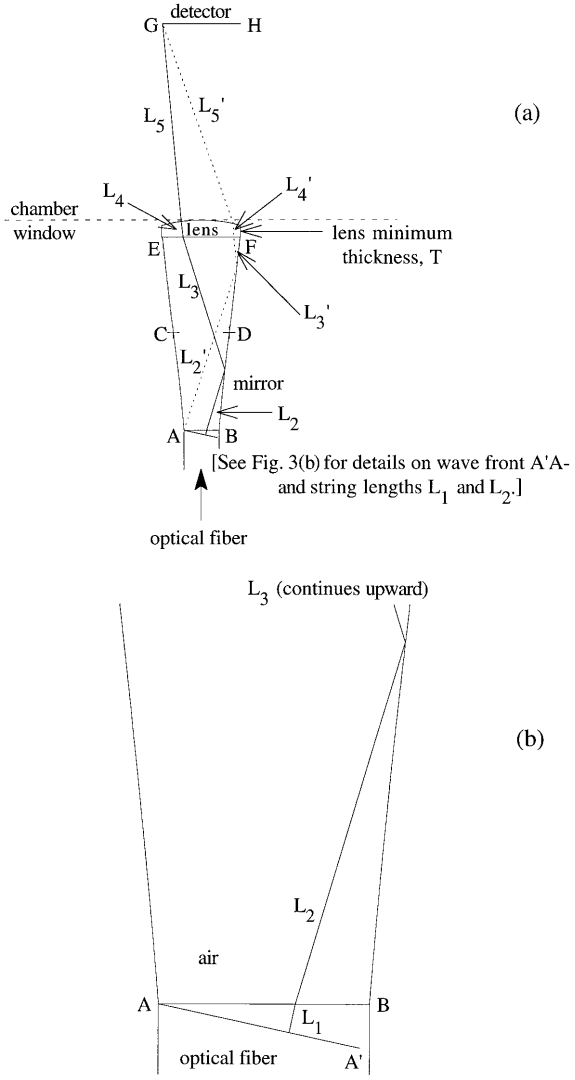

Fig. 3. Design of the lens–mirror nonimaging unit, in 2D cross section. The reflector extends from entrance aperture AB to exit aperture EF. The lens has minimum (edge) thickness T. In this particular exercise, the lens is taken to have the same refractive index as the fiber. Rays emerge from fiber tip AB into air over an angular range of $\pm 25.0°$. $A'A$ is the wave front of entering extreme rays. The reflector design proceeds according to the method of strings as described in the text. String lengths are denoted by L: (a) full view; (b) zoom on entrance aperture to show details of string lengths in that region.

from the exit aperture inward: All points on the mirror must reflect edge rays from point A exactly to target edge G. The mirror section FD is therefore the arc of a rotated ellipse, the foci of which are A and G. Point F of the exit aperture is determined by the requirement that it lie at the closest point of approach to the target, i.e., a distance of 5 mm from the plane of EF to the plane of GH [Fig. 2(a)].

Continuing the elliptical arc from point F, one reaches a point, D, where the angle, which an extreme ray from point A makes with the optic axis, would have to exceed the maximum permissible value of 25°. Hence a different shape is needed between points D and B. That shape must take all rays emitted from the extreme entrance wave front $A'A$ and focus them to detector edge G. Therefore DB is simply a rotated parabolic arc, the focus of the parabola being point G and the parabola axis being at an angle of 25° relative to the optic axis. In the language of nonimaging concentrators, our solution is a synthesis of the compound parabolic concentrator and the compound elliptical concentrator[1] in the sense that were the roles of target and source reversed, we would have an ideal radiation concentrator for a small source at a finite distance and a highly restricted exit angle at the absorber.

An alternative method of derivation is the method

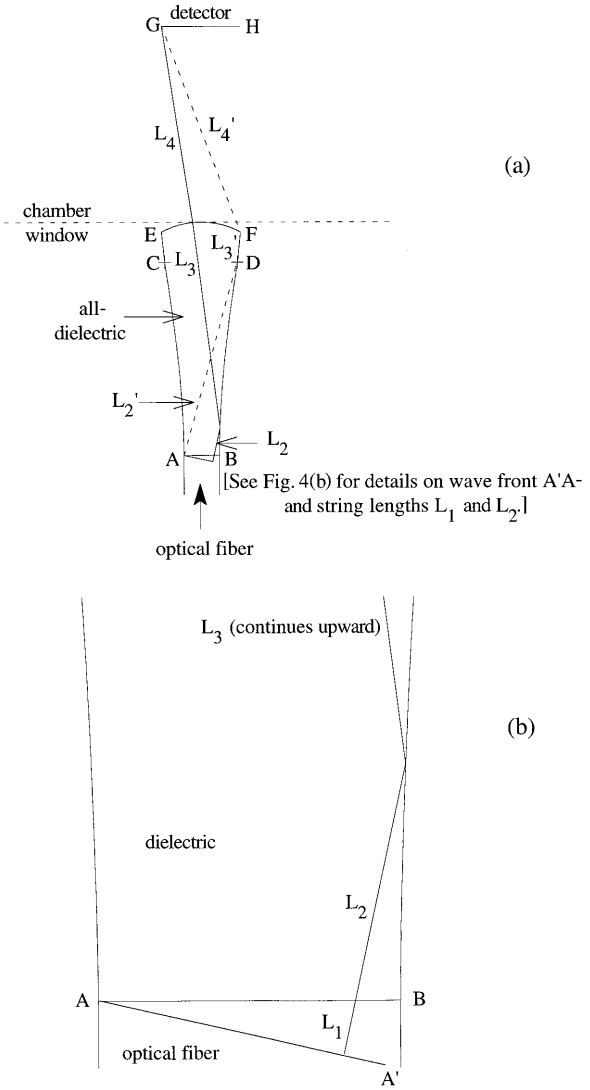

Fig. 4. Design of the all-dielectric nonimaging unit, in 2D cross section. The side profile extends from entrance aperture *AB* to *EF*, and a spherical cap at *EF* creates the exit aperture. In this particular exercise, the irradiator is taken to have the same refractive index as the fiber. Rays enter the irradiator from fiber tip *AB* over an angular range of ±11.55°. *A′A* is the wave front of entering extreme rays. Reflector design proceeds according to the method of strings as described in the text. String lengths are denoted by *L*: (a) full view; (b) zoom on entrance aperture to show details of string lengths in that region.

of strings,[1] a fusion of the edge-ray principle with Fermat's principle, whereby the design is such that the optical path length along the incident wave front of edge rays, to the target extreme, is constant for all edge rays. With reference to Fig. 2 with string lengths denoted by L, this means that for any ray from $A'A$,

$$nL_1 + L_2 + L_3 = \text{constant}, \tag{1}$$

where n is the refractive index of the fiber. For any ray emerging from source edge A at an angle $<25°$,

$$L_2' + L_3' = \text{constant}. \tag{2}$$

Table 1. Representative Device Characteristics for Several All-Mirror Designs[a]

Reflector Depth (mm)	Radiative Efficiency
63.34	0.952
33.37	0.931
20.55	0.906
16.96	0.886
13.56	0.856
8.43	0.770

[a]Fiber active diameter = 0.9 mm.

The constants in Eqs. (1) and (2) are the same.

The practical problem with this class of design is device depth. For example, to deliver 100% of the rays to the target (in the 2D design), the mirror depth must be 463 mm, clearly grossly impractical for real fiber-optic installations. However, consider the pragmatic trade-off where one purposely introduces a small sacrifice in collection efficiency in exchange for a shallower reflector.

One strategy for gaining a markedly more compact unit at the expense of slightly reduced radiative efficiency is designing the illuminator for a fictitiously large (virtual) target, e.g., of linear dimension 2.1 mm instead of 2.0 mm. Illuminator depth here is determined by the extreme ray from wave-front point A′ (Fig. 2) that reflects off the mirror at point B and is directed to detector edge G. Because the angle formed by the straight line BG with the optic axis is small, a modest oversizing of the virtual target offers a substantial reduction in device depth. A few sample designs are summarized in Table 1. These results, along with the results in all tables presented here, include skew-ray losses. The designs cited in Table 1 incur a skew-ray rejection of only 2–3.5%.

The advantage of the all-mirror design is ease of fabrication, relative to units that are molded from dielectrics,[5] and the low infrared absorptive losses that are possible when gold coatings are used. Still, device depth is sufficiently great that more compact alternatives should be considered.

4. Lens–Mirror Combination

As realized in Ref. 8, the depth of maximum-performance nonimaging reflectors designed for small fields of view can be reduced significantly by the introduction of a lens at the exit aperture. One then tailors the mirror according to the edge-ray principle to ensure maximum radiative efficiency. The resulting optical system can satisfy the constraints imposed here, at acceptable compactness. An example is illustrated in Fig. 3. The lenses considered here would be fabricated from the same material as the fiber, although this need not be a limitation. Our treatment extends that of Ref. 8 in treating a target at a finite (rather than at infinite) distance, and at a limited entrance angle (rather than ±90°).

Select a lens of given radius of curvature R and given minimum edge thickness T (assuming the lens

Table 2. Representative Device Characteristics for a Few Lens–Mirror Designs

Exit Aperture Diameter (mm)	Lens Radius of Curvature (mm)	Lens Minimum Thickness (mm)	Total Depth (mm)	Radiative Efficiency
2.03	3.70	0.30	4.40	0.990
1.94	3.10	0.30	3.43	0.979
1.85	3.00	0.30	3.13	0.961
2.03	3.71	0.10	4.50	0.993
1.94	3.16	0.10	3.59	0.983
1.85	3.01	0.10	3.29	0.964
2.10 (truncated *V*-cone)	4.24	0.30	4.85	0.959

cannot be cut razor sharp at its edges). Invoking the edge-ray principle, we determine the two sections, FD and DB, of the right-hand-side mirror profile (Fig. 3). The upper section, FD, is tailored to the edge rays emitted from the fiber edge A at angles $<25°$ relative to the optic axis. Reflector FD ensures that, for given lens characteristics, these extreme rays are all focused to target edge G. From the method of strings, we require that

$$L_2' + L_3' + nL_4' + L_5' = \text{constant}'. \tag{3}$$

The lower reflector DB is tailored to the rays emitted from extreme wave front A′A, according to

$$nL_1 + L_2 + L_3 + nL_4 + L_5 = \text{constant}'. \tag{4}$$

For a narrow range of lens parameters, the reflectors turn out to be very well approximated by a *V*-cone (i.e., by a *V*-trough in 2D cross section). The advantage is the relative ease and accuracy with which a *V*-cone mirror can be fabricated relative to curved 3D contours.

These nonimaging devices cannot be made arbitrarily shallow. The reason is that beyond a certain degree of compactness (depending upon lens properties), the caustic of edge rays falls in front of the reflector rather than behind it. This would imply that points on the reflector must simultaneously accommodate two different edge rays, which from Snell's Law is impossible. Hence ray rejection must ensue.

As for the pure-mirror case analyzed in Section 3, one can reduce device depth by purposely designing for an oversized target: compactness is earned at the expense of ray rejection. These designs were also considered. Table 2 lists a few representative cases. In all instances listed, skew-ray rejection is in the range 0.5–1%.

The results summarized in Table 2 highlight the degree to which superior compactness can be achieved relative to the pure-mirror designs of Section 3. For certain realistic values of system parameters, the reflectors turn out to be well approximated by a truncated *V*-cone (i.e., by a truncated *V*-trough in a 2D cross section), which can reduce fabrication difficulties and expense.

Table 3. Representative Device Characteristics for Two All-Dielectric Designs

Exit Aperture Diameter (mm)	Exit Aperture Radius of Curvature (mm)	Total Depth (mm)	Radiative Efficiency
1.998	6.46	17.51	1.000
2.020	3.03	7.95	0.997

5. All-Dielectric Total-Internal-Reflection Designs

All-dielectric (monolithic) total-internal-reflection radiation concentrators were developed in Ref. 9. We consider their illumination analogs. We skip the analysis of dielectric devices with a flat (disk-shaped) exit aperture (the rigorous analog of the pure-mirror devices discussed in Section 3), because of excessive depth. An attractive and practical alternative is available. Adopt the observation that, in a pure-dielectric unit, a lens–profile combination permits superior compactness at no sacrifice in optical performance. In fact, the lower optical path length within the dielectric should reduce absorptive losses.

Since rays emerging from the fiber into the dielectric irradiator of the same refractive index undergo no refraction, the restricted entrance angle at entrance aperture AB is $\pm 11.55°$. Only at exit aperture EF will rays increase dramatically in angular extent (relative to the local normal to the lens surface).

Applying the edge-ray principle to our problem and referring to Fig. 4, we start by choosing a lens-shaped entrance aperture with radius of curvature R, and then determine the profiles *FD* and *BD* from the principle of constant optical path length for edge rays. For the edge rays from point A that enter at $<11.55°$, the string lengths must satisfy

$$nL_2' + nL_3' + L_4' = \text{constant}''. \tag{5}$$

For the edge rays from wave front $A'A$ that leave the fiber at precisely 11.55°, the corresponding relation is

$$nL_1 + nL_2 + nL_3 + L_4 = \text{constant}''. \tag{6}$$

These pure-dielectric devices cannot be made arbitrarily shallow. One problem is that of the caustic of edge rays being formed within the device, as noted for the lens–mirror units in Section 4. Another problem is ensuring no radiation leakage. Namely, every ray striking the side profile must be within the dielectric's critical angle θ_c ($\sin \theta_c = 1/n$), relative to the local normal, to respect total internal reflection. The more compact of the two devices listed in Table 3 corresponds to the shallowest unit that respects both these constraints. Skew-ray rejection for these designs is negligibly small.

6. Alternative Nonimaging Designs

There are alternative nonimaging design strategies that could be adapted to the fiber-optic problem delineated here for all-dielectric[10] and lens-only[11] de-

signs, with the latter calling for a lens that is detached from the fiber. With radiative efficiencies for the devices presented here being near 98%, clearly there is little room for improvement in optical performance. Furthermore we find no practical advantage (such as superior compactness) for these alternatives.

For example, the detached lens-only invention of Ref. 11 demands two precision alignments: the fiber with the lens and the lens with the target. With the optical device attached to the optical fiber, the designs considered here call for only a single alignment with the target, as well as for it to be smaller and more portable.

We find that the all-dielectric tailored, edge-ray devices of Ref. 10, when adapted to accommodate a restricted entrance angle and a target at a finite distance, are comparable in size and performance to the designs detailed in Section 5. These designs are composed of an aspheric exit aperture shape tailored to one family of extreme rays, with the side profiles tailored to the other family of edge rays, such that total internal reflection is always observed. With no improvement in device compactness, and comparable radiative efficiency to the units detailed in Section 5, we found no particular motivation for detailed presentation of our findings here.

7. Discussion

First, the practical problems of deep nonimaging optical systems that plagued the commercial development of solar energy concentrators and building lighting systems are markedly diminished in fiber-optic applications because the dimension with which the reflector or dielectric profiles scale is the fiber diameter, which here is <1 mm. For example, an irradiator that is, say, 20 mm deep is easy to fabricate and not problematic in actual installations.[5] In contrast, consider a solar concentrator with an absorber of 1-m diameter and comparable relative dimensions. Its depth would be near 20 m, which is clearly unwieldy and impractical. Furthermore the lens in a lens–mirror design, or the dielectric in the all-dielectric system, would be unreasonably large (and heavy).

Second, the flux map emerging from an optical fiber might not be uniform (a uniform flux map was assumed for our designs). The emerging flux might be peaked toward small angles owing to the increase in absorption within the fiber as the incidence angle increases, and because the light input itself is sometimes inhomogeneous and peaked toward small angles.[4,5] We are not aware of any systematic design principles for nonuniform incident flux distributions. So the best we can do for now is to design for uniformly emitting light sources (albeit restricted in angular extent). Once design tools for inhomogeneous light sources are developed, their major advantage will probably be to permit the use of more compact devices (since skew-ray rejection is close to negligible).

Third, we note that skew-ray rejection is impressively small for all the devices developed here, and exceptionally low for the lens–mirror and pure-dielectric (lens-profile) units. The superior skew-ray acceptance of the lens–mirror and pure-dielectric designs, compared with the pure-mirror illuminators, probably arises from their possessing a relatively larger fraction of directly emitted rays, i.e., relatively more rays reach the device exit aperture without undergoing any reflection. In certain applications where the target is not a standard square photodiode, but rather a circular target, skew-ray rejection will increase by $\sim$1–3% (depending on the design and the dimensions) relative to the values cited here. In all cases, skew-ray rejection remains, at most, at the level of a few percent.

Fourth, only geometric, as opposed to material, losses have been accounted for. Absorptive losses will typically be negligibly small because of (a) the high reflectivity of gold mirror coatings in the infrared coupled with the small average number of reflections incurred in our designs, and (b) the low absorptivity of the dielectrics considered here over lengths of the order of a few millimeters. The major optical losses will stem from Fresnel reflections at dielectric–air interfaces. These can be reduced markedly with existing antireflective coatings[5] and are minimally dependent on the details of our geometric designs.

Fifth, what are the improvements and the advantages in optical efficiency and overall system design for our nonimaging devices compared with a conventional imaging alternative? Consider the use of a section of an ellipsoidal mirror to accomplish the same objective. The two foci of the ellipse are placed at the center of the fiber tip and the center of the detector. In the ellipsoidal configurations of greatest radiative efficiency, 70–80% of the power emitted from the fiber strikes the target, which has been confirmed experimentally.[5]

The advantage of higher radiative efficiency in nonimaging systems, relative to imaging designs, decreases as the numerical aperture of the fiber decreases. Imaging systems incur lower aberrations for smaller fields of view. These points are inherent to both imaging and nonimaging systems.[1] Similarly, in applications where the field of view into, and hence exiting from, the fiber exceeds the low value considered here, the advantage of our nonimaging designs will increase.

As a fast analytic estimate, consider the extreme case of far-field radiation detection, with the radiation emerging from the fiber being limited to angular range $\pm\phi$, and with the requirement that a relatively small angular range $\pm\theta_a$ be produced by our optical device ($\theta_a \ll \phi$). The pure-reflective imaging design would be a parabola with the center of the fiber as its focus. The superiority in the radiative efficiency of the nonimaging system would then be a factor of $\cos^{-2}\phi$.[1,7] That superiority is slightly greater for the exercise analyzed in Sections 2–5 due to (i) the detector being near-field and hence the reflector being ellipsoidal and (ii) an effective θ_a that is not small

compared with ϕ. The same conclusions pertain to a single spherical lens system as well.

The boost in optical performance from nonimaging solutions is not as dramatic as earlier advances in radiation concentration,[1,7] which related to maximum numerical aperture systems. The more limited boost for optical fibers, however, is still far from negligible, and is inherently limited by the fiber's numerical aperture.

Sixth, the physical extent of the imaging system (be it mirror- or lens-based) will typically be much larger than our compact, proximate nonimaging systems. In fact, in assessing the feasibility of these nonimaging solutions versus existing conventional designs, the boost in radiative efficiency will probably be secondary relative to the practical advantages of (i) a substantially smaller optical system in the distance between fiber, optical element, and target; (ii) significantly smaller optical elements; and (iii) requiring one, rather than two, precision alignments.

Seventh, our nonimaging designs can accommodate realistic fabrication constraints. For example, it often turns out that a truncated *V*-cone mirror is far easier to produce, with greater contour precision, than any mirror with curvature in its 2D cross section. In the lens–mirror combination, for certain values of the lens radius of curvature, minimum lens end thickness, and exit aperture diameter, the mirror turns out to be very well approximated by a truncated *V*-cone (truncated *V*-trough in 2D). Similarly, a truncated *V*-cone dielectric profile is often much easier to fabricate than curved profiles. Likewise, in our all-dielectric designs, there are values of exit surface radius of curvature and diameter for which the side profiles are essentially straight lines in a 2D cross section. Namely, one has the flexibility to tailor device characteristics to manufacturing limitations at little or no sacrifice in optical efficiency.

The tool box of nonimaging optics offers a rich spectrum of design options that can be tailored to the material properties and the experimental configuration particular to different applications. Illuminators can be produced from mirrors only, monolithic dielectric units, or lens–mirror combinations. The dielectric materials used in these irradiators and lenses need not be the same material as that of the fiber, although for convenience and practicality, the dielectric materials we used in our design exercises were the same as the fiber. At radiative efficiencies approaching 100%, these compact, readily fabricated, nonimaging designs appear to provide superior, operative alternatives to conventional imaging solutions.

We thank Abraham Katzir of Tel Aviv University for bringing the details of the infrared fiber optic applications to our attention and for encouragement in the development of these solutions.

References

1. W. T. Welford and R. Winston, *High Collection Nonimaging Optics* (Academic, San Diego, Calif., 1989).
2. A. Katzir, *Lasers and Optical Fibers in Medicine* (Academic, San Diego, Calif., 1993).
3. D. Bunimovich, R. Kellner, R. Krska, A. Mesica, I. Paiss, U. Schiesl, M. Tacke, K. Taga, and A. Katzir, "A system for monitoring and control of processes based on IR fibers and tunable diode lasers," J. Mol. Struct. **292,** 125–132 (1993).
4. S. Shalem, S. A. German, and A. Katzir, "Optical properties of silver-halide core/clad IR fibers," in *Medical and Fiber Optic Sensors and Delivery Systems*, G. Orellana, A. V. Scheggi, N. I. Croitoru, M. Miyagi, and H. J. Sterenborg, eds., Proc. SPIE **2631,** 216–225 (1995).
5. A. Katzir, Department of Physics, Tel Aviv University, Tel Aviv, Israel (personal communication, 1996).
6. H. Ries and A. Rabl, "Edge-ray principle of nonimaging optics," J. Opt. Soc. Am. A **11,** 2627–2632 (1994).
7. A. Rabl, *Active Solar Collectors and Their Applications* (Oxford U. Press, New York, 1985).
8. M. Collares-Pereira, A. Rabl, and R. Winston, "Lens–mirror combinations with maximal concentration," Appl. Opt. **16,** 2677–2683 (1977).
9. X. Ning, R. Winston, and J. O'Gallagher, "Dielectric totally internally reflecting concentrators," Appl. Opt. **26,** 300–305 (1987).
10. R. P. Friedman and J. M. Gordon, "New optical designs for ultra-high flux infrared and solar energy collection: monolithic dielectric tailored edge-ray concentrators," Appl. Opt. **35,** 6684–6691 (1996).
11. J. C. Miñano and J. C. González, "New method of design of nonimaging concentrators," Appl. Opt. **31,** 3051–3060 (1992).